



ORIGINAL ARTICLE

Elaboration of nickel-impregnated over hexagonal mesoporous materials and their catalytic application



M. Laribi *, K. Bachari, M. Touati

Centre de Recherche Scientifique et Technique en Analyses Physico-Chimiques (C.R.A.P.C), BP 248, Alger RP 16004, Alger, Algeria

Received 5 December 2011; accepted 13 March 2012
Available online 20 March 2012

KEYWORDS

Hexagonal mesoporous silicas;
Characterization;
Textural property

Abstract Hexagonal mesoporous silicas with different nickel contents have been synthesized and characterized by several techniques such as N₂ physical adsorption, elemental analysis, XRD, TEM and temperature programmed reduction (TPR). In fact, the nickel-impregnated over hexagonal mesoporous silicas showed both high activity and high selectivity for Friedel–Crafts alkylations of benzene with benzyl chloride. The kinetics of the reaction over these catalysts have been investigated and the reaction has been extended to other substrates like toluene, *p*-xylene, anisole, naphthalene and methylnaphthalene.

© 2012 Production and hosting by Elsevier B.V. on behalf of King Saud University. This is an open access article under the CC BY-NC-ND license (<http://creativecommons.org/licenses/by-nc-nd/3.0/>).

1. Introduction

Friedel–Crafts alkylations comprise a very important class of reactions which are of common use in organic chemistry. These reactions are habitually catalyzed by Lewis acids in li-

quid phase (Olah, 1973), and the substitution of liquid acids by solid acid catalysts is a challenging task. The alkylation of benzene (Bz) by benzyl chloride (BzCl) is interesting for the preparation of substitutes of polychlorobenzenes used as dielectrics. In homogeneous phase this reaction is catalyzed at the industrial scale by AlCl₃, FeCl₃, BF₃, ZnCl₂ and H₂SO₄ (Olah, 1973; Olah et al., 1985; Commandeur et al., 1991). The new environmental legislation pushes for the replacement of all liquid acids by solid acid catalysts which are environmentally more friendly catalysts and which lead to minimal pollution and waste (Clark et al., 1994; Cao et al., 1998). Indeed, several solid acid catalysts have already been proposed which are efficient catalysts such as Fe-modified ZSM-5 and H-β zeolites; Fe₂O₃ or FeCl₃ deposited on micro-, meso- and macro-porous (Choudhary et al., 2002a); Fe-containing mesoporous molecular sieves materials (He et al., 1998; Bachari et al., 2004); Ga- and Mg-oxides and chlorides derived from Ga–Mg-hydrotralicite (Choudhary et al.,

Abbreviations: Bz, benzene; BzCl, benzyl chloride; TEOS, tetraethyl orthosilicate; EtOH, ethanol; MeO, methanol; HCl, chloride acid; NaOH, sodium hydroxide; XRD, X-ray diffraction; TEM, transmission electron microscopy; TPR, temperature programmed reduction; GC–MS, gas chromatography coupled with mass spectroscopy.

* Corresponding author. Tel./fax: +213 21247406.

E-mail address: mourad_laribi@yahoo.fr (M. Laribi).

Peer review under responsibility of King Saud University.



Production and hosting by Elsevier

2002b); Ga-SBA-15 (El Berrichi et al., 2006); Ga-HMS (Bachari and Cherifi, 2006a); transition metal chloride supported mesoporous SBA-15 (Bachari and Cherifi, 2006b); supported thallium oxide catalysts (Choudhary and Jana, 2001); Sb supporting K10 (Deshpande et al., 2001); Si-MCM-41-supported Ga_2O_3 and In_2O_3 (Choudhary et al., 2000a); alkali metal salts and ammonium salts of kegglin-type heteropolyacids (Izumi et al., 1995); ion-exchanged clays (Cseri et al., 1995); Cu-HMS (Bachari and Cherifi, 2006c); solid superacids based on sulfated ZrO_2 (Koyande et al., 1998) for the benzylation of benzene and other aromatic compounds. The discovery of the new family of mesoporous silica molecular sieves with pore diameters in the 2.0–10 nm range, designated as M41S, is of considerable interest for heterogeneous catalysis and material science (Kresge et al., 1992; Beck et al., 1992). Depending on the synthesis conditions, different phases could be obtained, like the hexagonal phase MCM-41, the cubic one MCM-48 as well as the lamellar compound MCM-50. Furthermore, another pathway was proposed by Tanev et al. (1994) to prepare mesoporous silicas at room temperature by neutral templating route (S^0I^0). In this case, the organic surfactant is not quaternary ammonium cation but a primary amine, and the assembly involves hydrogen-bonding interactions between neutral primary amines and neutral inorganic precursors. These materials denoted as HMS (hexagonal mesoporous silica), reveal excellent catalytic capacity for macromolecular reactions and suggest new opportunities for transition metal incorporation into silica frameworks. In the present work, we report the elaboration of hexagonal mesoporous silicas with different nickel contents and their application as catalysts for Friedel–Crafts alkylations of benzene.

2. Experimental

2.1. Materials

Samples were synthesized with hexadecylamine (HDA, Aldrich), tetraethyl orthosilicate (TEOS, Aldrich), nickel–nitrate ($\text{Ni}(\text{NO}_3)_2 \cdot 6\text{H}_2\text{O}$, Merck), ethanol (EtOH, Rhône-Poulenc), methanol (MeOH, Aldrich), chloride acid (HCl, Aldrich), benzene (Bz, Aldrich), benzene chloride (Bz, Aldrich) and sodium hydroxide (NaOH, Aldrich).

2.2. Catalysts preparation

The HMS material was prepared following the pathway reported by Tanev et al. (1994). In a representative preparation, HDA (0.3 mol) was added to a solution containing water (36 mol) and EtOH (7 mol) and the mixture was stirred until homogeneous. Then 1 mol of TEOS was added under vigorous stirring. This solution was then stirred at room temperature for 24 h to obtain the product. The solid was recovered by filtration, washed with distilled water, and air-dried at 393 K for 24 h. Organic molecules occluded in the mesopores were removed by solvent extraction. The dried precursor was dispersed in EtOH (5 g/100 ml) and the mixture was refluxed under vigorous stirring for 2 h. The resultant was then filtered and washed with cold ethanol. The extraction procedure was repeated twice before drying the samples at 393 K in an oven. Finally the samples were calcined at 823 K in air for 6 h. Impregnated mesoporous materials Ni (wt%)/HMS with Ni

(%) = 2 and 8 are prepared as follows: the amount of nickel nitrate is added to 5 g of pure HMS and 50 g of MeOH. The mixture is agitated at ambient temperature during 2 h, the solvent is then rapidly evaporated under vacuum and the solid is calcined under air at 723 K overnight at a heating rate of 1 K min^{-1} .

2.3. Characterization of the samples

The chemical compositions of the samples were determined by a combination of wet chemical methods and atomic absorption spectrometry (HITACHI Z 800). Adsorption/desorption experiments using N_2 were carried out at 77 K on a NOVA 2000 porosimeter (Quantachrome) instrument. Powder X-ray diffraction patterns were recorded on SIEMENS D500 diffractometer with $\text{Cu-K}\alpha$ radiation. Transmission electron microscopy (TEM) measurements were performed with a Philips CM10 electron microscope operated at 100 kV. Temperature programmed reduction (TPR) experiments were performed with a TPDRO1100 apparatus from Thermo Quest CE Instruments. Temperature programmed reduction (TPR) experiments were performed with a TPDRO1100 apparatus from Thermo Quest CE Instruments. For the TPR measurements the calcined samples were pelletised, ground and sieved. Sieve fractions between 425 and 850 μm were placed in a fixed bed reactor and used for analysis. A flow containing 5% hydrogen and 95% argon (Hoek Loos) was passed downward through the catalyst bed at a rate of 20 ml min^{-1} . After water removal from the outcoming flow (mol sieves) hydrogen consumption was measured using a tungsten thermal conductivity detector.

2.4. Catalytic testing

The benzylation reactions over a series of impregnated nickel over mesoporous silicas catalysts were carried out in a magnetically stirred glass reactor (25 cm^3) fitted with a reflux condenser, having a low dead volume, mercury thermometer and arrangement for continuously bubbling moisture free nitrogen N_2 (flow rate = $30 \text{ cm}^3 \text{ min}^{-1}$) through the liquid reaction mixture, at the following reaction conditions: reaction mixture Bz/BzCl = 15 ml of moisture-free liquid aromatic compound (or 2.5 ml of moisture-free aromatic compound mixes with 12.5 ml of moisture-free solvent) + 1.0 ml of BzCl, amount of catalyst = 0.1 g and reaction temperature = 353 K. The reaction was started by injecting BzCl in the reaction mixture, containing catalyst and aromatic compound with or without solvent. Measuring quantitatively the HCl evolved in the reaction by acid–base titration (by absorbing the HCl carried by N_2 in a 0.1 M NaOH solution containing phenolphthalein indicator) followed the course of the reaction (Choudhary et al., 2000b). Samples were analyzed periodically on a gas chromatograph (HP-6890) equipped with an FID detector and a capillary column RTX-1 (30 m \times 0.32 mm i.d.). The products were also identified by GC–MS (HP-5973) analysis.

3. Results and discussion

3.1. Characterization

The results of the chemical composition and characteristics of the catalysts are given in Table 1. The nickel compositions of

Table 1 Chemical composition and characteristics of the catalysts.

| Sample | Chemical analysis | | Surface area ($\text{m}^2 \text{g}^{-1}$) | Pore volume (ml g^{-1}) | d (nm) ^b |
|-------------|-------------------------|-----------------------|---|------------------------------------|-----------------------|
| | Theor. content Ni (wt%) | Real content Ni (wt%) | | | |
| HMS | – | – | 1170 | 0.96 | – |
| Ni (2%)/HMS | 2.0 | 1.88 | 870 | 0.90 | < 2.8 |
| Ni (8%)/HMS | 8.0 | 7.69 | 812 | 0.83 | 11.3 |

^b The diameter of nickel particles obtained by transmission electron microscopy (TEM).

the solids corresponded relatively well to those fixed for the synthesis. Most of the values of the specific surface areas of the solids were larger than $800 \text{ m}^2 \text{ g}^{-1}$, which were typical mesoporous materials. When the nickel content increased, they decreased slightly. In the other hand, a very narrow pore size distribution, centered on 3 nm, was calculated from nitrogen physisorption data. Furthermore a very high pore volume ($0.96 \text{ cm}^3 \text{ g}^{-1}$) was measured. This high value reflects the very high surface area of the support. The XRD patterns of the solids showed a broad peak at $2\theta = 2.2$ (Fig. 1) characterizing a mesoporous material not well-crystallized. The intensity of the peak decreased slightly when the nickel content increased showing that the addition of nickel has not a negative effect on the crystallinity. At the same time, XRD diffractograms of the solids in the $10\text{--}80^\circ$ (2θ) range displaying the diffraction pattern characteristic of nickel oxide (JCPSD Card no: 47-1049) are presented in Fig. 2. Ni (8%)/HMS display intense and well resolved NiO peaks, indicating that relatively large nickel oxide particles are present. However, the broad onsets of these peaks reveal that smaller nickel oxide particles are also present. With the Ni (2%)/HMS catalyst only very weak reflections are obtained, indicating that exclusively very small nickel oxide particles have formed. The size of these particles could not be determined accurately, because the signal to noise ratio was too low, even after extended analysis times. TEM analyses of the catalysts indicated that large nickel oxide particles had formed with the catalyst Ni (8%)/HMS (11.3 nm), whereas no large nickel oxide particles could be visualized with the Ni (2%)/HMS catalyst (Table 1). Indeed, line broadening of the diffraction peaks in the XRD patterns of the calcined catalysts demonstrates that with both catalysts very small

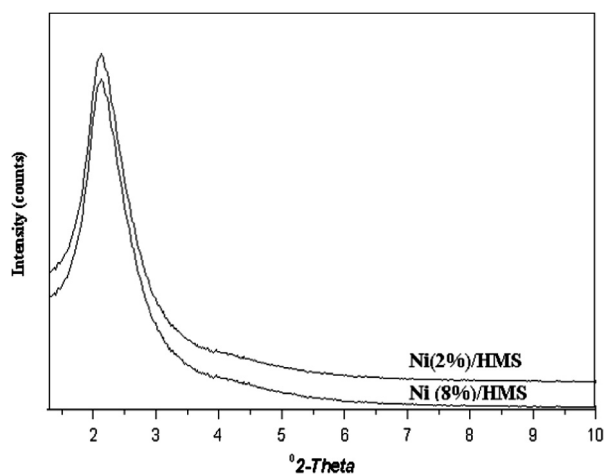


Figure 1 XRD patterns of the Ni (%) /HMS catalysts in the domain of $1\text{--}10^\circ$ (2θ).

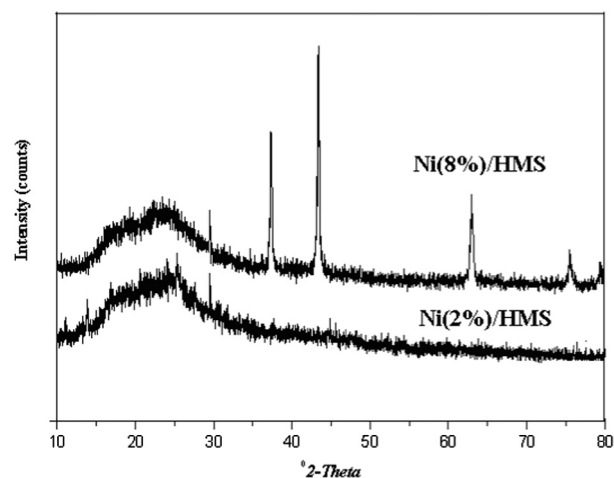


Figure 2 XRD patterns of the Ni (%) /HMS catalysts in the domain of $10\text{--}80^\circ$ (2θ).

(< 2.8 nm) nickel oxide particles were present, which could conceivably be situated at the internal surface. With the catalyst Ni (2%)/HMS the presence of exclusively small nickel oxide particles can be inferred from the diffractogram (Fig. 2) in which only broad, low-intensity peaks are visible; whereas with the catalyst Ni (8%)/HMS narrow, intense peaks reveal that large (> 10 nm) particles are codeposited as well. The same trends were found with TEM: no nickel oxide particles could be visualized with the Ni (2%)/HMS catalyst, whereas large particles were found with the Ni (8%)/HMS catalyst. Reduction plots of the catalysts are given in Fig. 3. To

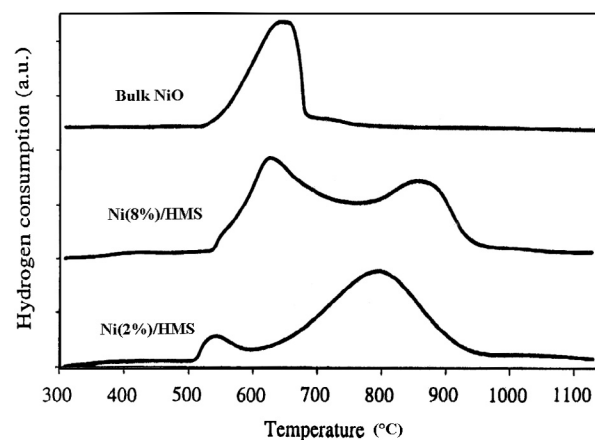


Figure 3 Reduction patterns of Ni (%) /HMS catalysts and bulk NiO.

Table 2 Catalytic properties of the catalysts in the benzylation of Bz with BzCl at 348 K, Bz/BzCl = 15 and $m_{\text{cat}} = 0.1$ g.

| Catalyst | Time (min) ^a | Selectivity (%) | | Apparent rate constant k_a ($\times 10^4 \text{ min}^{-1}$) |
|-------------|-------------------------|------------------|--------------------|---|
| | | Diphenyl methane | Polybenzyl benzene | |
| HMS | – | – | – | – |
| Ni (2%)/HMS | 483.4 | 100.0 | – | 86.2 |
| Ni (8%)/HMS | 262.3 | 100.0 | – | 174.8 |

^a Time required for the complete conversion of benzyl chloride.

Table 3 Catalytic activities of Ni (8%)/HMS at different temperatures: 343, 348 and 353 K, Bz/BzCl = 15 and $m_{\text{cat}} = 0.1$ g.

| Temperature (K) | Time (min) ^a | Selectivity (%) | | Apparent rate constant k_a ($\times 10^4 \text{ min}^{-1}$) |
|-----------------|-------------------------|------------------|--------------------|---|
| | | Diphenyl methane | Polybenzyl benzene | |
| 343 | 376.4 | 100.0 | – | 115.2 |
| 348 | 262.3 | 100.0 | – | 174.8 |
| 353 | 129.8 | 99.3 | 0.7 | 345.6 |

^a Time required for the complete conversion of benzyl chloride.

enable comparison a reduction plot of bulk NiO, obtained from $\text{Ni}(\text{NO}_3)_2 \cdot 6\text{H}_2\text{O}$ by calcinations at the temperature of 923 K for 6 h, is also included. Indeed, TPR analysis was used to attain information about the reducibility of the deposited nickel oxide of the catalysts. In the case of the catalyst Ni (8%)/HMS two large reduction stages are observed. The large low-temperature reduction stage coincides with the reduction of bulk NiO, indicating the presence of nickel oxide with a bulk character. As a consequence, the nickel oxide particles associated with this reduction stage have to be rather large. Thus, the second reduction stage is associated with the presence of very small nickel oxide particles, stabilized by the HMS framework. The catalyst Ni (2%)/HMS mainly contains small nickel oxide particles, which is demonstrated by the high temperature of reduction. Nevertheless, the very small low-temperature reduction peak points to the presence of some slightly enlarged particles too, which are not observed with the other characterization techniques. These particles are most likely located at the external surface of the HMS grains. In fact, these results are in agreement with the results of the XRD and TEM gotten previously.

3.2. Catalytic performances of Ni (%) /HMS materials in the benzylation of benzene

A comparison of the catalytic properties of the solids tested is presented in Table 2. The pure silicic compound (HMS) was totally inactive. The other compounds showed an activity increasing with the nickel content. However, the selectivity to diphenylmethane remains constant.

3.3. Reaction kinetics

The kinetic data for the benzene benzylation reaction in excess of Bz (stoichiometric ratio Bz/BzCl = 15) over the Ni (8%)/HMS catalyst (0.1 g) could be fitted well to a pseudo-first-order

rate law: $\log[1/(1-x)] = (k_a/2.303)(t-t_0)$ where k_a is the apparent first-order rate constant, x the fractional conversion of BzCl, t the reaction time and t_0 the induction period corresponding to the time required for reaching equilibrium temperature. A plot of $\log[1/(1-x)]$ as a function of the time gives a linear plot over a large range of BzCl conversions. The effect of temperature on the reaction rate was studied by conducting the reaction at 343, 348, and 353 K under the standard reaction conditions (stoichiometric ratio Bz/BzCl = 15 and 0.1 g catalyst). The results showed that the catalytic performances of the catalyst strongly increased with the reaction temperature (Table 3). By contrast, the selectivity of diphenylmethane remains approximately constant. The activation energy estimated thus obtained was 96.7 kJ mol^{-1} . In fact, this value can probably suggest that no interference of diffusional limitations is existed. Two Bz/BzCl ratios have been investigated. The results obtained are reported in Table 4. It appears that the stoichiometric ratio between Bz and BzCl has a strong influence on the selectivity to diphenyl methane. With a low ratio, the secondary reactions to dibenzylbenzenes and tribenzylbenzene were favored. Results showing the influence of different substituent groups attached to aromatic benzene nucleus on the conversion of BzCl in the benzylation of corresponding substituted benzenes at 353 K over the Ni (2%)/HMS catalyst are presented in Table 5. According to the classical mechanism of the Friedel–Crafts type acid catalyzed benzylation reaction, the benzylation of an aromatic compound is easier if one or more electron donating groups are present in the aromatic ring (Olah, 1973). The first-order rate constant

Table 4 Influence of the stoichiometric ratio between Bz and BzCl chloride for the benzylation of benzene at 348 K over Ni (8%)/HMS catalyst.

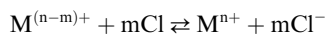
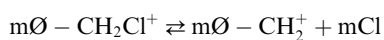
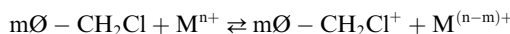
| Benzene/benzyl chloride ratio | Time (min) ^a | Selectivity (%) | |
|-------------------------------|-------------------------|------------------|--------------------|
| | | Diphenyl methane | Polybenzyl benzene |
| 5 | 370.4 | 69.5 | 30.5 |
| 15 | 262.3 | 100.0 | – |

^a Time required for the complete conversion of benzyl chloride.

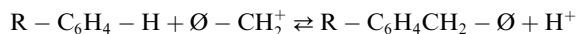
Table 5 Catalytic properties of substituted benzenes and substituted naphthalene at 353 K over Ni (8%)/HMS catalyst, Bz/BzCl = 15 and $m_{\text{cat}} = 0.1$ g.

| Substituent | Apparent rate constant k_a ($\times 10^4 \text{ min}^{-1}$) | Reaction products (selectivity (%)) |
|---------------------|---|---|
| Benzene | 345.6 | Diphenylmethane (99.3%) |
| Toluene | 334.0 | Para-benzylated (89%), Ortho-benzylated (9%), Meta-benzylated (2%) |
| <i>p</i> -Xylene | 327.3 | 2,5-Di-methyl diphenylmethane (>99%) |
| Anisole | 305.2 | Para-benzylated (87%), Ortho-benzylated (11%), Meta-benzylated (2%) |
| Naphthalene | 282.5 | – |
| 2-Methylnaphthalene | 224.5 | – |

for the benzylation of benzene and substituted benzenes is in the following order: benzene > toluene > *p*-xylene > anisole. This indicates that, for this catalyst, the reaction mechanism is different from that for the classical acid catalyzed benzylation reactions. In fact, the probable redox mechanism for the activation of both BzCl and Bz by these catalysts leading to the benzylation of benzene reaction is proposed:



where M = Ni; $n = 2$ and $m = 1$; O = phenyl.



The redox mechanism is similar to that proposed earlier for the benzene benzylation and acylation reactions (Choudhary and Jana, 2001; Cseri et al., 1995; Briio et al., 2000). Furthermore, in order to rule out the influence of a steric effect on the rate of reaction, we have applied the Taft relation (March, 1985). According to this relation when a steric effect influences the reaction, there is a linear relation between the rate and the parameter E_s values considered to be representative of the size of the substituting group of the studied aromatic compounds. Using the E_s parameter tabulated by Charton (1975) we have shown that such a relation did not exist. Furthermore, the catalyst Ni (8%)/HMS is always active and selective for larger molecules like naphthenic compounds such as methylnaphthalene (Table 5). The large pores of the mesoporous support permit the conversion of these molecules that could not be done on other supports.

3.4. Effect of solvent

In the aim to appreciate the role of solvent in benzylation of benzene by nickel-containing samples with BzCl, the reaction was carried out with different solvents, such as dichloroethane and *n*-heptane. The reaction conditions and the results of benzene benzylation with Ni (8%)/HMS catalyst are presented in Table 6. The conversion of the catalyst decreased in the presence of aprotic solvent due to the interaction of negative charge or the electron lone pair of solvent with acidic sites of the catalyst. The reaction rate is highest in the absence of any solvent. It is decreased when the solvent (via dichloroethane and *n*-heptane) is used, the decrease is quite large when *n*-heptane is used as a solvent but it is small for dichloroethane as a solvent. The observed solvent effect on reaction rate is ex-

Table 6 Effect of solvent on the conversion of BzCl at 353 K in the benzylation of Bz over Ni (8%)/HMS, Bz/BzCl = 15 and $m_{\text{cat}} = 0.1$ g.

| Solvent | Time (min) ^a | Apparent rate constant k_a ($\times 10^4 \text{ min}^{-1}$) |
|-------------------|-------------------------|---|
| Without solvent | 129.8 | 345.6 |
| Dichloroethane | 132.5 | 342.1 |
| <i>n</i> -Heptane | 138.8 | 338.8 |

^a Time required for the complete conversion of benzyl chloride.

Table 7 Effect of recycling of the catalysts in the benzylation of Bz with BzCl at 353 K over Ni (8%)/HMS catalyst, Bz/BzCl = 15 and $m_{\text{cat}} = 0.1$ g.

| Catalyst | Time (min) ^a | Selectivity (%) | | Apparent rate constant k_a ($\times 10^4 \text{ min}^{-1}$) |
|--------------|-------------------------|------------------|--------------------|---|
| | | Diphenyl methane | Polybenzyl benzene | |
| Fresh | 129.8 | 99.3 | 0.7 | 345.6 |
| First reuse | 137.1 | 98.3 | 1.7 | 340.1 |
| Second reuse | 142.7 | 97.1 | 2.9 | 334.7 |

^a Time required for the complete conversion of benzyl chloride.

pected because of the competitive adsorption of both the reactants and the solvent on the catalyst and because of the high solubility of the polymer in dichloroethane and little solubility of the polymer in *n*-heptane. Indeed, when the solubility of the polymer in a particular solvent is low, the polybenzyl formed on the catalyst surface is not removed from the surface and this is expected to deactivate the catalyst due to the occupation of its active sites by the product formed during the initial reaction. The results show that between the two solvents, dichloroethane is a better solvent for the benzylation reaction.

3.5. Recycling of the catalysts

The stability of the catalysts has been studied by running the reaction successively with the same catalyst (Ni (8%)/HMS) under the same conditions without any regeneration between two runs. The reaction was first run under the standard conditions (Bz/BzCl = 15, $T = 353$ K) to the complete conversion of BzCl. Then after a period of 10 min another quantity of BzCl was introduced in the reaction mixture leading to the same ratio. After the achievement of the second run, the same protocol was repeated second time. The results, presented in Table 7, showed that the catalyst could be used several times in the benzene benzylation process without a significant change of its catalytic activity.

4. Conclusion

Hexagonal mesoporous silicas with different nickel contents show amazing activities for the Friedel–Crafts alkylations of Bz with BzCl. More interesting is the observation that this catalyst is at all times active and selective for large molecules like naphthenic compounds such as methylnaphthalene and it can also be reused in the Friedel–Crafts alkylations of benzene with benzyl chloride for several times.

References

- Bachari, K., Cherifi, O., 2006a. *J. Mol. Catal. A: Chem.* 253, 187–191.
- Bachari, K., Cherifi, O., 2006b. *J. Mol. Catal. A: Chem.* 260, 19–23.
- Bachari, K., Cherifi, O., 2006c. *Catal. Commun.* 7, 928–930.
- Bachari, K., Millet, J.M.M., Benaichouba, B., Cherifi, O., Figueras, F., 2004. *J. Catal.* 221, 55–61.
- Beck, J.S., Vartuli, J.C., Roth, W.J., Leonowicz, M.E., Kresge, C.T., Schmitt, K.D., Chu, C.T.W., Olson, D.H., Sheppard, E.W., McCullen, S.B., Higgins, J.B., Schlenker, J.L., 1992. *J. Am. Chem. Soc.* 114, 10834–10843.

- Brio, K., Bekassy, S., Agai, B., Figueras, F., 2000. *J. Mol. Catal. A: Chem.* 151, 179–184.
- Cao, J., He, N., Li, C., Dong, J., Xu, Q., 1998. *Mesopor. Mol. Sieves* 117, 461–467.
- Charton, B., 1975. *J. Am. Chem. Soc.* 97, 1552–1556.
- Choudhary, V.R., Jana, S.K., 2001. *J. Catal.* 201, 225–235.
- Choudhary, V.R., Jana, S.K., Kiran, B.P., 2000a. *J. Catal.* 192, 257–261.
- Choudhary, V.R., Jana, S.K., Kiran, B.P., 2000b. *Catal. Lett.* 64, 223–226.
- Choudhary, V.R., Jana, S.K., Mamman, A.S., 2002a. *Microporous Mesoporous Mater.* 56, 65–71.
- Choudhary, V.R., Jana, S.K., Narkhede, V.S., 2002b. *Appl. Catal. A: Gen.* 235, 207–215.
- Clark, J.H., Cullen, S.R., Barlow, S.J., Bastock, T.W., 1994. *J. Chem. Soc. Perkin Trans.*, 1117–1130.
- Commandeur, R., Berger, N., Jay, P., Kervenal, J., 1991. *Eur. Pat.* 0422 986.
- Cseri, T., Bekassy, S., Rizner, S., Figueras, F., 1995. *J. Mol. Catal. A: Chem.* 98, 101–107.
- Deshpande, A.B., Bajpai, A.R., Samant, S.D., 2001. *Appl. Catal. A: Gen.* 209, 229–235.
- El Berrichi, Z., Cherif, L., Orsen, O., Fraissard, J., Tessonnier, J.P., Vanhaecke, E., Louis, B., Ledoux, M.J., Pham-Huu, C., 2006. *Appl. Catal. A* 298, 194–202.
- He, N., Bao, S., Xu, Q., 1998. *Appl. Catal. A: Gen.* 169, 29–36.
- Izumi, Y., Ogawa, M., Urabe, K., 1995. *Appl. Catal. A: Gen.* 132, 127–140.
- Koyande, S.N., Jaiswal, R.G., Jayaram, R.V., 1998. *Ind. Eng. Chem. Res.* 37, 908–913.
- Kresge, C.T., Leonowicz, M.E., Roth, W.J., Beck, J.C., 1992. *Nature* 359, 710–712.
- March, J., 1985. *Advanced Organic Chemistry*, third ed. Wiley/Interscience, New York.
- Olah, G.A., 1973. *Friedel–Crafts Chemistry*. Wiley/Interscience, New York.
- Olah, G.A., Prakash, G.K.S.J., Sommer, J., 1985. *Superacids*. Wiley/Interscience, New York.
- Tanev, P.T., Chibwe, M., Pinnavaia, T.J., 1994. *Nature* 368, 317–321.